Spectroscopic Assessment of Secondary and Tertiary Structure in Myelin Basic Protein†

Cynthia S. Randall and Robert Zand*

Biophysics Research Division, Macromolecular Research Center, and Department of Biological Chemistry, The University of Michigan, Ann Arbor, Michigan 48109

Received July 3, 1984

ABSTRACT: Myelin basic protein conformation and hydrophobicity, along with the protein's behavior in the presence of the fluorescent probe 6-(*p*-toluidino)-2-naphthalenesulfonate, have been studied by using Fourier transform infrared (FT-IR) and Raman spectroscopy. The FT-IR and Raman spectra provided compelling evidence for the presence of a small amount of β structure, ca. 25%, in the aqueous solution and solid-state forms of myelin basic protein. The enhanced fluorescence and shift in the emission maximum of 6-(*p*-toluidino)-2-naphthalenesulfonate when bound to myelin basic protein are consistent with the presence of at least one hydrophobic region in the molecule. Loss of the fluorescence enhancement in the presence of denaturing agents indicates that native myelin basic protein has a folded structure in solution. All of the results provide support for conformational predictions derived from the application of Edmundson wheels to the primary structure.

Interest in the structure and behavior of myelin basic protein (MBP) can be ascribed to its implication in the etiology of multiple sclerosis (Einstein et al., 1972; Cammer et al., 1978; Whitaker et al., 1980). The unique amino acid composition of MBP [see Martenson (1980) and references cited therein] and the controversy surrounding its in vivo structure and function have also contributed to the numerous investigations of MBP conformation. The solution properties of MBP have already been extensively studied with techniques such as light scattering (Liebes et al., 1975), ultracentrifugation (Liebes et al., 1976; Smith, 1980), circular dichroism (Block et al., 1973; Liebes et al., 1975; Swann & Li, 1979), and nuclear magnetic resonance (Liebes et al., 1975; Deber et al., 1978; Campagnoni et al., 1978). However, the analyses and interpretation of these results have not provided a totally coherent picture, and some of the most recent results, in particular, have added to the conflict.

Many of the reported studies have concluded that MBP has little, if any, organized structure in aqueous solution, behaving essentially as a random coil. In contrast, theoretical predictions of MBP secondary structure (Martenson, 1981; Stoner, 1984) indicate that MBP should have regions of repetitive secondary structure; in particular, β structure and β turns appear to have a high probability. Recent investigations using high-resolution NMR (Mendz et al., 1982), along with results obtained from immunological studies (Whitaker, 1982; Fritz & Chou, 1983), suggest that MBP has a greater degree of ordered structure than previously assigned. Moreover, studies from this laboratory have revealed an in vitro hydrolytic capability of MBP which obeys saturation kinetics (Zand & Agrawal, 1980). The presence of an active-site catalysis is supportive of a greater degree of three-dimensional stability in MBP than has been recognized to date.

The present study was undertaken with the objectives of ascertaining the degree of stable secondary and tertiary structure in MBP and of identifying particular types of secondary structure within the protein. The binding of 6-(*p*-toluidino)-2-naphthalenesulfonate (TNS), a fluorescent probe specific for hydrophobic regions, was used to determine the existence of such interactions in MBP. In addition, Fourier transform infrared spectroscopy (FT-IR) and Raman spectroscopy were used to characterize MBP conformation in solution and in the solid state. The results of these experiments and their significance are presented in the following sections.

Materials and Methods

Myelin basic protein was isolated and purified from bovine brains and spinal cords according to the procedure of Deibler et al. (1972). Purity was determined by gel electrophoresis. Deuterated MBP was prepared by repeatedly dissolving and freeze-drying purified solid samples in D_2O.

Fourier transform infrared studies were carried out with a Digilab 20C spectrometer interfaced to a digital computer. Solution spectra were obtained by using a BaF_2 variable path-length cell. Protein concentrations were generally in the range of 1–2% (w/v); unless otherwise noted, the cell path length was adjusted to 150 μm. Oriented films of MBP were prepared by casting protein solutions on silver chloride plates and evaporating to dryness with unidirectional stroking. Polarizers set at 0° and 90° with respect to the incoming light were used to determine dichroism in the MBP films. Sample and solvent spectra were recorded under conditions of moderate resolution (2 cm^{-1}); the instrument was purged with liquid nitrogen during data collection. The number of scans taken depended on sample preparation and concentration; 100–1000 scans were found to be adequate for most solution spectra. Wavenumber positions reported here are considered accurate to ± 2 cm^{-1}.

Raman spectra were recorded with a Spex spectrometer interfaced to a computer system. The excitation source at 5145 Å was an argon ion laser. Solid and aqueous solution (5%) MBP samples were sealed in melting point capillary tubes which were aligned 90° to the laser beam. The spectral slit width was 200 μm. The power at the sample was maintained at approximately 150 mW. Depending on the sample, spectra

† This work was supported in part by a grant from the National Science Foundation (BNS 7904381).

* Address correspondence to this author at the Institute of Science and Technology, The University of Michigan.

0006-2960/85/0424-1998$01.50/0

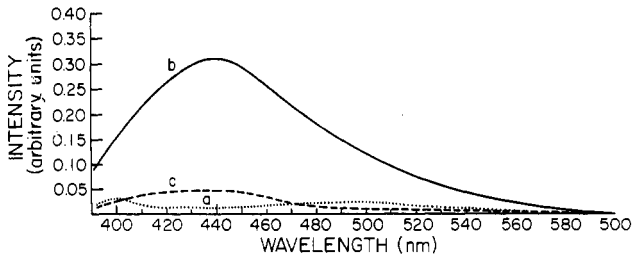

FIGURE 1: Fluorescence emission spectra of TNS (2.8×10^{-5} M) in 0.05 M sodium acetate at pH 4.5. The exciting wavelength is 350 nm. (a) TNS; (b) equimolar TNS and MBP; (c) TNS and MBP with 8 M urea, after correction for background fluorescence of TNS alone in 8 M urea.

were obtained by signal averaging five scans acquired at a rate of 0.5 cm^{-1}/s (solid samples) or 20 scans acquired at a rate of 1 cm^{-1}/s (solution sample). Spectral frequencies are reported to ± 2 cm^{-1}.

The fluorescent probe 6-(*p*-toluidino)-2-naphthalenesulfonate potassium salt was purchased from Sigma and stored in the dark at 4 °C. Solutions of TNS in the desired solvents were prepared just prior to use; concentrations were verified from the ultraviolet absorbance spectra (McClure & Edelman, 1966). Fluorescence measurements were made with a modified Aminco-Bowman spectrophotofluorometer equipped with a high-intensity xenon lamp. All samples were studied in 1-cm path-length quartz cuvettes. Titrations of MBP with TNS were performed by adding increments of the dye to a fixed volume of protein solution, as well as to an identical volume of solvent without protein. Emission spectra from 400 to 600 nm were recorded with an excitation wavelength of 350 nm. All spectra reported here have been corrected.

Results

Binding of TNS. As shown in Figure 1, aqueous solutions of TNS in the absence of MBP exhibit very weak fluorescence. The emission spectrum is quite broad, with a maximum centered around 500 nm. In contrast, the fluorescence intensity of TNS in the presence of MBP is markedly increased, accompanied by a narrowing of the bandwidth and a shift in the maximum to higher energy. The emission maximum of the MBP–TNS complex is now centered at 443 nm. This value falls within the range of maxima reported for other TNS–protein complexes (McClure & Edelman, 1966; Turner & Brand, 1968). In the presence of 8 M urea, a generally accepted protein unfolding reagent, the fluorescence intensity is dramatically reduced. Similar effects were also observed in the presence of 6 M guanidinium chloride, another common denaturant. This behavior is interpreted as a disruption of the hydrophobic interactions present in native MBP. Such interactions cannot be stabilized when folding is altered by denaturing agents.

The titration of MBP in TNS initially reflects relatively large increases in fluorescence intensity, as seen in curves a–c of Figure 2. Above a dye to protein ratio of 0.7, the intensity appears to increase only in small amounts, as shown in curves d and e of Figure 2. The apparent leveling off of fluorescence intensity may arise from a saturation effect. An alternative explanation would ascribe the observed behavior to an aggregation artifact; the ease of MBP self-association has been well documented (Liebes et al., 1975; Smith, 1980). We believe the latter possibility can be discounted here for the following reason: Optical density measurements were carried out at the exciting wavelength of 350 nm on the TNS–MBP complexes in the presence and absence of 8 M urea and exhibited less than 0.01 absorbance variation. This indicates that

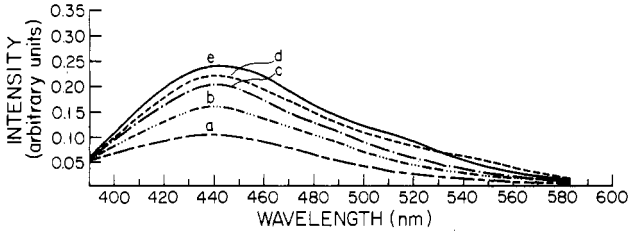

FIGURE 2: Fluorescence emission spectra of various TNS–MBP complexes in 0.05 M sodium acetate, pH 4.5. The exciting wavelength is 350 nm. Increments of TNS were added to MBP of initial concentration 3.4×10^{-5} M to obtained the following [TNS]/[MBP] ratios: (a) 0.14; (b) 0.42; (c) 0.69; (d) 0.98; (e) 1.25.

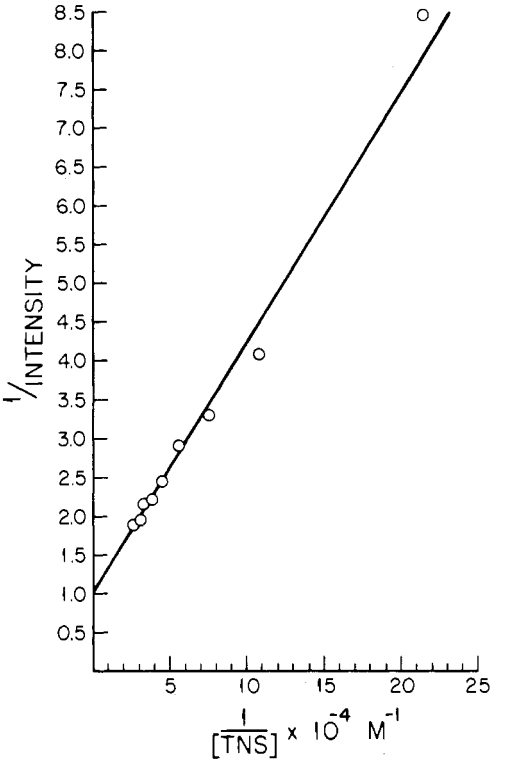

FIGURE 3: Fluorescence titration of MBP with TNS, performed in 0.05 M sodium acetate at pH 4.5. The exciting wavelength is 350 nm. The initial concentration of MBP is 1.4×10^{-4} M.

at these dye and protein concentrations, aggregation does not distort the observed fluorescence spectra (Parker, 1968). It is worth noting that under other conditions, this assumption may not be valid; when MBP is added to a large molar excess of TNS at pH 8.0, immediate precipitation is observed.

The dissociation constant for the TNS–MBP complex was determined by using the equation of McClure & Edelman (1967):

$$\frac{1}{I} = \frac{1}{I_0} + \left(\frac{K_{d,app}}{I_0}\right)\left(\frac{1}{[F_0]}\right)$$

where I is the observed fluorescence intensity, I_0 is the maximum possible fluorescence at infinite dye concentration, $K_{d,app}$ is the apparent dissociation constant, and $[F_0]$ is the molar concentration of the fluorophore. A plot of $1/I$ vs. $1/[F_0]$ (Figure 3) yields I_0 and $K_{d,app}$ from the slope and intercept, respectively. Application of this equation to the titration data for MBP yields a value of $K_{d,app}$ of 2.1×10^{-5} M, in good agreement with a previous report (Feinstein & Felsenfeld, 1975).

An attempt was made to also characterize the behavior of MBP–TNS complexes in less polar environments by the use of nonaqueous solvents. By subtracting out the fluorescence

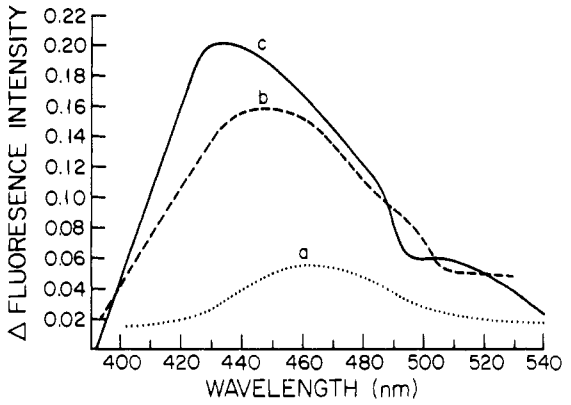

FIGURE 4: Fluorescence emission spectra of equimolar TNS–MBP complexes, 3.4×10^{-5} M, in aqueous/organic solvent systems. The exciting wavelength is 350 nm. The fluorescence intensity of TNS alone in the various solvent systems was subtracted to obtain the above spectra: (a) 60% CF_3CH_2OH; (b) 10% $(CH_3)_2SO$; (c) 60% $(CH_3)_2SO$.

of a TNS blank in the solvent system of interest, the hydrophobic contribution of MBP could be estimated. As can be seen in Figure 4, both trifluoroethanol and dimethyl sulfoxide (Me_2SO) perturb the folding of MBP. The latter solvent is particularly effective in its ability to influence MBP hydrophobicity. Striking effects of Me_2SO on MBP were also observed in the infrared spectrum and in ^1H NMR studies. In these experiments, the concentration of MBP was 10–100 times greater than those used in the fluorescence measurements. Even in dilute solutions of MBP, where intermolecular effects should be reduced, Me_2SO appears to promote the existence of a more effective hydrophobic binding site for TNS, as demonstrated by the observed blue shift and increased intensity.

The use of infrared spectroscopy to explore the conformation of proteins and polypeptides is well documented (Schellman & Schellman, 1964; Susi, 1972). The basis for the assignment of conformational states are the vibrational frequencies arising from the peptide backbone. These include the N–H stretch near 3300 cm^{-1}, the C=O stretch or amide I region from 1600 to 1680 cm^{-1}, and the N–H deformation or amide II region from 1500 to 1570 cm^{-1}. The amide I and amide II bands are particularly sensitive to different forms of protein secondary structure, which are reflected in the observed frequencies of the band maxima (Miyazawa & Blout, 1961; Krimm, 1962).

Table I: Summary of Infrared and Raman Data on MBP

data	sample medium	frequency (cm^{-1})[a]	assignment
infrared	D_2O solution	1658, 1651, 1639, 1634 (sh)	amide I
	CF_3CH_2OH solution	1654 (sh), 1649, 1635 (vw)	amide I
	$(CH_3)_2SO$ solution	1686 (sh), 1677, 1673, 1668, 1660 (vw)	amide I
	dehydrated film	1657, 1628 (vw)	amide I
		1547 (sh), 1538, 1528 (sh), 1517 (sh)	amide II
Raman	solid state[b]	1669, 1661, 1653 (sh)	amide I
		1277, 1241, 1235	amide III
		853, 828	tyrosine
	solid state[c]	1285 (sh), 1273, 1234, 1225	amide III
	H_2O solution	1683 (sh), 1671, 1662	amide I
		1250, 1232	amide III
		855, 835	tyrosine

[a] sh and vw represent shoulder and very weak, respectively. [b] Obtained at room temperature. [c] Obtained at 4 °C.

The strong absorbance of the H_2O bending mode occurs in the same region as the amide I band and presents experimental problems for studies of proteins in aqueous solution. Although successful subtraction of the H_2O contribution has been reported (Lavialle et al., 1982; Vincent et al., 1984), the present experimental conditions dictated the use of D_2O instead. While D_2O does not absorb strongly in the amide I region, it does have inherent limitations with respect to the interpretation of the spectra obtained (Calvin et al., 1959). Trifluoroethanol and dimethyl sulfoxide also do not absorb strongly in the amide I region and were used to characterize the behavior of MBP in nonaqueous environments. Representative solution spectra are shown in Figure 5; band positions and assignments are summarized in Table I.

Because the amide I modes for the α helix and random coil should appear at almost the same frequency, ca. 1650 and 1655 cm^{-1}, respectively (Susi et al., 1967), it is difficult to make definitive distinctions between the two conformations from the above infrared data alone. However, previous circular dichroism studies strongly indicate that the α-helix conformation does not make a major contribution to MBP structure in aqueous media (Liebes et al., 1975; Swann & Li, 1979). The infrared spectrum of MBP in D_2O (Figure 5a) is interpreted as being characteristic of a predominantly random-coil

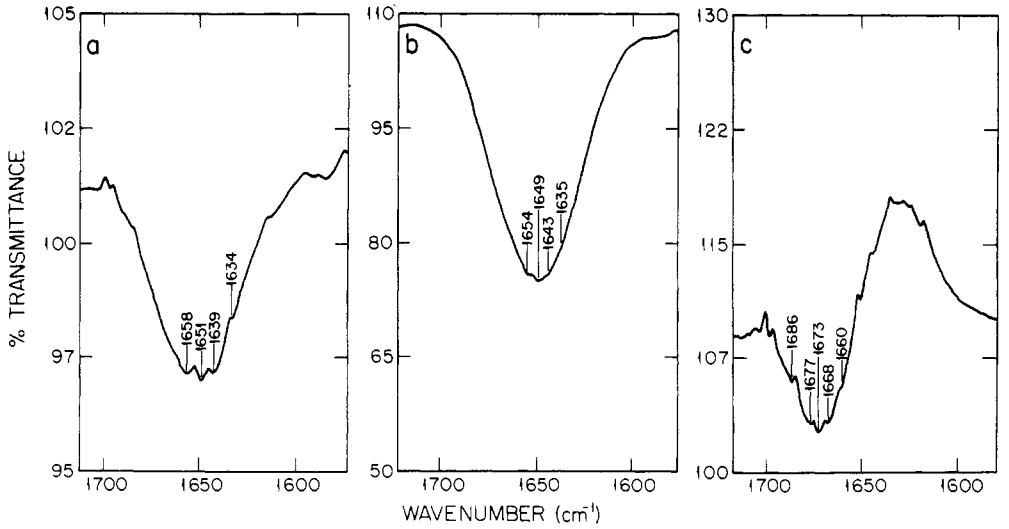

FIGURE 5: Amide I band in infrared spectra of MBP in various solvents: (a) D_2O; (b) CF_3CH_2OH; (c) $(CH_3)_2SO$ (obtained with cell path length of 50 μm).

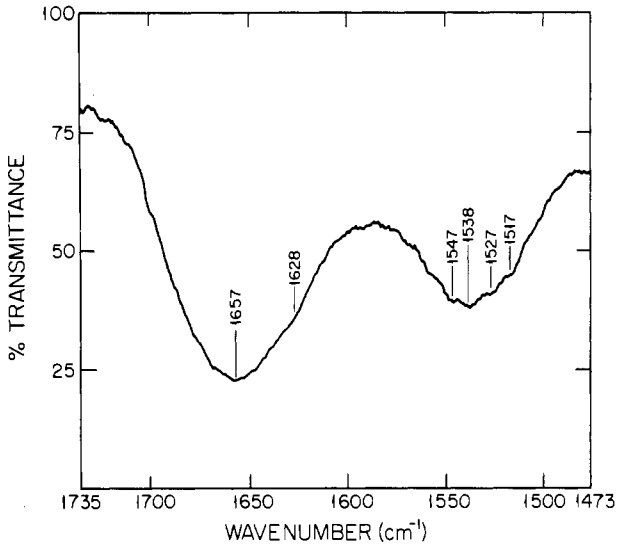

FIGURE 6: Amide I and II bands in infrared spectrum of dehydrated MBP film.

structure. However, the inflection visible at 1634 cm^{-1} is ascribed to the presence of a small amount of antiparallel β-sheet structure (Timasheff & Susi, 1966; Ruegg et al., 1975).

Trifluoroethanol is known to promote α-helix formation in MBP (Liebes et al., 1975). In 100% trifluoroethanol (Figure 5b), the amide I region of MBP is narrowed and shifted to lower energy with respect to the absorption in D_2O. While calculations of helical content from CD data indicate about 70% of MBP exists as an α helix in trifluoroethanol, the infrared data obtained in this solvent also indicate the presence of some antiparallel β-sheet conformation with respect to the inflection observed at 1635 cm^{-1}.

Although aggregation effects limited the infrared study of MBP in dimethyl sulfoxide, the data that were obtained for the amide I region (Figure 5c) differ from the spectra obtained in D_2O or trifluoroethanol. Of particular note is the appearance of an absorption maximum near 1670 cm^{-1}. Previous ^1H NMR studies carried out on MBP peptide fragments in Me_2SO-d_6 showed significant differences from spectra obtained in D_2O (Margetson et al., 1981; Sadikot & Moore, 1983). This behavior was attributed to the stabilization of β-turn structures by this solvent. While care should be exercised in extrapolating the behavior of isolated peptides to those of the intact protein, the amide I feature near 1670 cm^{-1} is tentatively attributed to the presence of β-turn conformations. However, because the amide I vibrational frequencies of some β-turn types overlap with those of α helix and β-pleated sheets, this assignment cannot be considered definitive (Krimm & Bandekar, 1980; Lagant et al., 1984).

The infrared spectrum obtained from films of MBP cast from aqueous solution is shown in Figure 6. The amide I and amide II regions are interpreted as indicating a significant amount of random-coil conformation, but the asymmetry of the bands implies the presence of other secondary structures. The shoulder on the amide I region at 1628 cm^{-1} and the shoulder on the amide II region at 1528 cm^{-1} are consistent with the presence of small amounts of antiparallel β–sheet structure. Additional shoulders on the amide II band at 1547 and 1517 cm^{-1} may be indicative of a small contribution from some helical structure.

The MBP films were not strongly oriented, and there was no substantial evidence of dichroism in the amide I and II regions, nor in the N–H stretching region at 3300 cm^{-1}. This observation is consistent with the belief that isolated MBP has

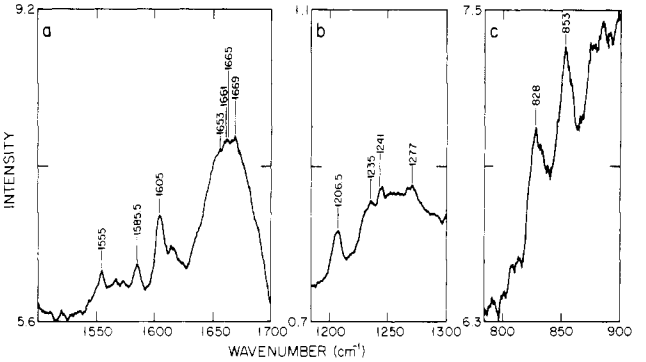

FIGURE 7: Raman spectral data for solid MBP obtained at room temperature: (a) amide I region; (b) amide III region; (c) tyrosine doublet region.

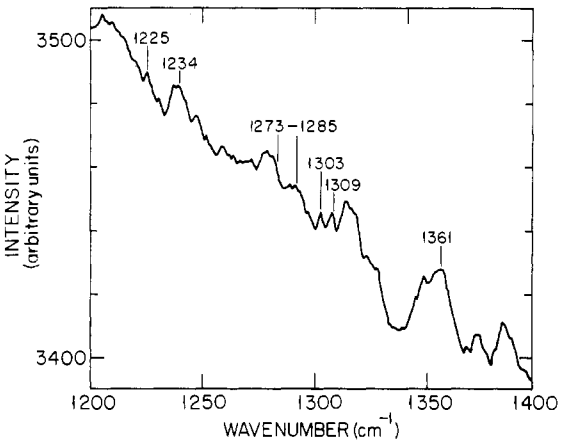

FIGURE 8: Raman spectral data for the amide III region of solid MBP obtained at 4 °C.

mostly unordered structure, but it does not rule out the existence of small amounts of β sheet and/or α helix.

Information derived from Raman spectra of proteins can complement the results obtained from infrared studies. Also, Raman spectra can be obtained directly from protein solutions in H_2O instead of using D_2O (Carey, 1982). The observed Raman frequencies for various MBP samples, and their tentative identifications, are listed in Table I.

Our efforts to obtain high-quality Raman data were complicated by the presence of a significant degree of background fluorescence. The origin of this effect is unclear since the MBP preparation showed no contamination on gel electrophoresis or high-pressure liquid chromatography (HPLC). It is, however, possible that a tightly bound low molecular weight impurity is present in our preparation. Similar results were obtained from MBP samples prepared and purified in other laboratories.

Raman spectra of solid MBP are shown in Figures 7 and 8. The broadness of the amide I band (Figure 7a) is indicative of the presence of several conformational forms. The maximum at 1669 cm^{-1} could be assigned to contributions from either random-coil or β-sheet secondary structures. In the amide III region (Figure 7b), the maximum at 1241 cm^{-1} is a strong indication of the presence of β-sheet regions (Pezolet et al., 1976; Hamodrakas et al., 1982). Pezolet et al. (1976) have developed a method for calculating the fraction of β structure from the Raman spectrum. This method utilizes the peak height intensities of the characteristic amide III band and the conformationally insensitive band at 1450 cm^{-1} which is associated with methylene bending modes; the relative peak height intensity of the 1240 cm^{-1} band shows a linear dependence on the amount of β structure known to be present

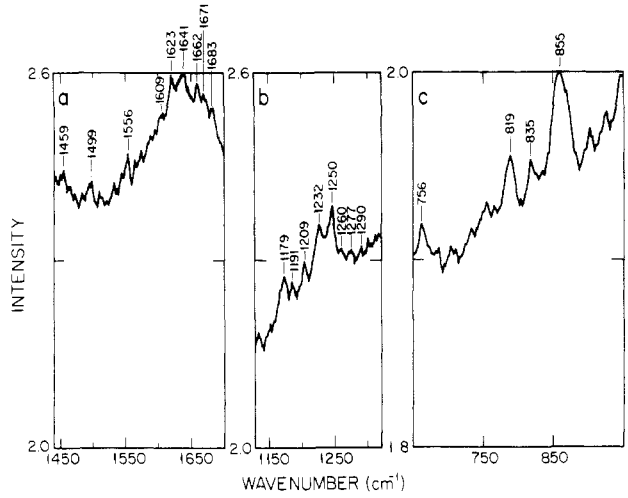

FIGURE 9: Raman spectral data for aqueous MBP (5% w/v) obtained at room temperature: (a) amide I region; (b) amide III region; (c) tyrosine doublet region.

in various proteins from X-ray crystallography. Using this relationship to analyze the Raman data on MBP yielded estimates of 21–25% β-sheet content. It should be noted that this method is only applicable when there is a well-defined amide III band occurring at 1240 ± 3 cm^{-1}. The estimates based on the above approach are in good agreement with the theoretical prediction of β sheet in MBP reported by Stoner (1984). The amide III region also shows a maximum at 1277 cm^{-1} which has tentatively been assigned to α-helix structure (Carey, 1982). At 4 °C (Figure 8), this band appears at 1273 cm^{-1}, while a band at ca. 1234 cm^{-1} is attributed to β-sheet structure.

Bands observed at 853 and 828 cm^{-1} in Figure 7c are assigned to ring vibrations of tyrosine. Yu et al. (1973) proposed that the intensity ratio of the two bands indicated whether such residues were exposed on a protein's surface or buried in its interior. Siamwiza et al. (1975) subsequently showed that the doublet intensity ratio is relatively insensitive to the environment of the phenyl ring but is sensitive to the nature of hydrogen bonding of the phenolic group or its ionization. If the phenolic oxygen acts as a proton donor to form a strong hydrogen bond in a hydrophobic environment, the I_{853}/I_{828} ratio should fall between 0.3 and 0.5. On the other hand, if the phenolic group forms a moderately strong hydrogen bond with water, the I_{853}/I_{828} ratio is predicted to be 1.25. The intensity ratio calculated from the spectral data was 1.4 ± 0.1, which supports the notion that the tyrosines in MBP are exposed.

In aqueous solution, the Raman spectrum of MBP (Figure 9) shows the broad amide I band similar to the band obtained from solid MBP. The amide III region exhibited maxima at 1250 and 1232 cm^{-1}, indicating the presence of both random and β conformations (Lippert et al., 1976). The intensity ratio of the tyrosine doublet I_{855}/I_{835} was 1.3 ± 0.1, which is quite close to the ratio obtained for the solid MBP. In either state, the tyrosine residues in MBP appear to be exposed on the surface rather than buried in a hydrophobic region.

The analysis of the Raman data on MBP must also consider the possibility of β turns. In contrast to α helices and β-pleated sheets, the spectroscopic characteristics of β-turn regions in proteins are still being developed (Bandekar & Krimm, 1980). To date, the best diagnostic evidence for β turns is an unusually high-frequency amide III band, in the region of 1290–1330 cm^{-1} (Krimm & Bandekar, 1980; Lagant et al., 1984). No particularly strong features were observed in this region in the Raman spectra of the various MBP samples; however, further experimental data are needed to determine the presence or absence of β turns in MBP under different conditions. On the basis of the present data, the β-sheet feature (not the β turn) appears to be the most significant component of ordered structure.

Discussion

The enhanced fluorescence intensity of TNS when bound to MBP in aqueous solvents in compelling evidence for the presence of a hydrophobic region on the folded MBP polypeptide surface. The dramatic diminution of fluorescence intensity when the TNS–MBP complex is placed in 8 M urea is a strong indication that the hydrophobic region is generated via the folding of the polypeptide backbone into a relatively stable three-dimensional structure. The infrared and Raman spectroscopic studies have, for the first time, provided physical evidence for the presence of a small amount of repetitive secondary structure and add additional support to the interpretation of the TNS binding data.

The presence of hydrophobic regions arising from protein folding in MBP may be essential in understanding the nature of this protein's interactions with other components of the myelin membrane. It is often argued that the association of MBP with certain phospholipids occurs mainly through electrostatic binding, with little perturbation of the lipid hydrocarbon chains. However, there is some evidence from NMR studies (Smith, 1982), as well as calorimetric and spin-label studies (Boggs & Moscarello, 1984), suggesting that hydrophobic interactions occur as well. Furthermore, Agrawal et al. (1982) have reported that during the purification of MBP from rat brain myelin, dissociation of endogenous lipids from MBP occurs only after the protein is treated with a strong denaturing agent such as urea. Such observations are consistent with the results reported here.

If the hydrophobic region is formed as a direct consequence of polypeptide chain folding, then the question of what type of folding is responsible can be legitimately asked. The linear sequence of bovine MBP has been represented with two-dimensional projections known as helical wheels in order to identify regions of helical and nonhelical potential. As detailed by Schiffer & Edmundson (1967), projections for α-helical segments in proteins usually show distinct hydrophobic arcs; these amino acids tend to be clustered in the $n \pm 3$, n, and $n \pm 4$ positions of adjacent helical turns to maximize intrahelical as well as interhelical interactions. Applying these criteria to MBP resulted in the identification of regions most likely to form α-helix structures:

Residues 35–45: hydrophobic arc formed by residues Phe-42, Ile-35, Leu-39, Phe-43, and Leu-36.

Residues 85–95: hydrophobic arc formed by residues Phe-88, Ile-92, Val-85, Phe-89, Val-93, and Val-86.

Residues 149–155: although this segment is too short to rigorously be considered an α helix, it does possess a hydrophobic arc with the required position distribution, i.e., residues Ile-152, Leu-149, Phe-153, and Leu-155.

In addition to the above regions, there are also several sequences which show hydrophobic clusters but do not satisfy the n, $n \pm 3$, and $n \pm 4$ required positions. Such segments may be helical in MBP and could participate in interhelical interactions, but they are less likely to form stable helices in solution when isolated. These regions are listed below:

Residues 12–29: hydrophobic arc formed by residues Phe-26, Met-19, and Tyr-12.

Residues 109–126: hydrophobic arc formed by residues Phe-113, Phe-124, Ala-117, and Leu-110.

Residues 126–143: hydrophobic arc formed by residues

Leu-140, Tyr-133, and Tyr-126.

Helical wheels for MBP folded into π helices also exhibit hydrophobic clusters in certain segments:

Residues 23–44: hydrophobic arc formed by residues Leu-39, Phe-26, and Ile-35.

Residues 61–82: hydrophobic arc formed by residues Ala-74, Ala-61, and Leu-70. Unlike the other arcs, this one is specific for the bovine MBP sequence. This particular segment is also of interest for its immunological properties: Sequence 64–73 is encephalitogenic in rabbit, while sequence 74–83 is encephalitogenic in rat. The latter determinant appears to be sequestered in intact MBP and requires fragmentation of the parent molecule in order to be recognized (Hashim, 1982).

Residues 111–132: hydrophobic arc formed by residues Ala-130, Ala-117, Tyr-126, and Phe-113.

Residues 133–154: hydrophobic arc formed by residues Phe-153, Leu-140, Leu-149, Ala-136, and Ala-145.

Residues 83–96: this segment is shorter than the others and thus may not define a true π helix. However, it does contain a hydrophobic arc of residues Val-93, Phe-89, and Val-85.

Strands of β structure were also analyzed with helical wheels. If the strands are assumed to be straight, the successive side chains will be located 180° apart from the backbone. Treating the primary structure of MBP in this fashion resulted in the formation of only two distinct hydrophobic clusters:

Residues 11–20: hydrophobic arc formed by Ala-16, Ala-14, and Tyr-12.

Residues 111–120: hydrophobic arc formed by Ala-117, Typ-115, and Phe-113.

However, β sheets have a tendency to twist; in this case, the angle between successive side chains may vary from 180° to 160°. When the latter angle is used to construct helical wheels for MBP, more than two hydrophobic regions are found:

Residues 12–22: hydrophobic arc formed by Ala-16, Ala-14, Tyr-12, and Met-19.

Residues 85–93: hydrophobic arc formed by Phe-88, Val-86, and Val-93. As previously stated, this fragment also has the potential to form the α helix. The theoretical predictions of Martenson (1981) indicate that the β structure has a greater probability of formation in this region, but experimental evidence to date is not conclusive.

Residues 109–117: hydrophobic arc formed by Leu-110, Ala-117, Trp-115, and Phe-113.

In addition to the above segments, there are several longer segments in the region containing residues 108–155 which will also form hydrophobic clusters when the wheels are extended outward. The introduction of twisted β sheets thus appears to promote further hydrophobic interactions in MBP, especially in the portion near the carboxyl-terminal end.

In surveying the helical wheels constructed for different types of secondary structure, there are certain amino acid sequences in MBP which appear especially likely to engage in hydrophobic interactions. One segment is located in the central portion of the molecule and includes Val-85, Val-86, Phe-88, Phe-89, Ile-92, and Val-93. Hydrophobic clusters involving most or all of these residues were found in the wheels of α-helix, π-helix, and twisted β-sheet structures. A second sequence contains Leu-110, Phe-113, Trp-115, and Ala-117. Residues from this group were found in hydrophobic clusters in the wheels of α-helix, π-helix, straight β-sheet, and twisted β-sheet structures. Residues Phe-113, Trp-115, and Ala-117 are also noteworthy as they comprise part of a nonapeptide fragment known to be encephalitogenic in guinea pig (Hashim, 1982).

The potential for the formation of regions of hydrophobicity by folding a linear polypeptide chain according to certain rules must be viewed as indicating that it can occur, not that it does occur. In the present instance, we view these predictive assessments merely as being consistent with the experimental results we have obtained. Additionally, these predictions help to identify specific regions within MBP which may participate in structural stabilization of the protein under conditions of biological interest.

The results of the present study suggest a reappraisal of the previously held assessment of MBP structure in an aqueous environment is necessary. This study plus the reports from other laboratories has provided sufficient evidence to support the concept of a more folded and stable structure for MBP. In turn, this reassessment of structure then permits a greater compatibility with the idea of an active site for esterolytic catalysis; it also supports the presence of at least one hydrophobic region capable of partial penetration into the myelin membrane lipid bilayer as well as interaction with esterolytic substrates.

While such substrates for MBP have not been identified in vivo, there is evidence supporting their existence. It is well-known that heme binds strongly to MBP (Liebes et al., 1975); recently, Vacher et al. (1984) have characterized this interaction in detail. The binding appears specific, with a 1:1 stoichiometry and a large association constant. Studies with peptide fragments of MBP indicate that maintenance of the bond between Phe-42 and Phe-43 is necessary for such binding to occur. Moreover, some nearby residues are highly homologous with a heme binding site of a mitochondrial cytochrome *b*. This information is consistent with the present helical wheel constructions for the α-helix structure in MBP, where a hydrophobic arc with the n, $n \pm 3$, and $n \pm 4$ distribution was seen in the sequence 35–45.

ACKNOWLEDGMENTS

We are grateful to Dr. Sofia Merajver, Keith Shaw, and Dr. Vaman Naik for obtaining the Raman spectra on our samples of myelin basic protein.

REFERENCES

Agrawal, H. C., O'Connell, K., Randle, C. L., & Agrawal, D. (1982) *Biochem. J. 201*, 39–47.

Bandekar, J., & Krimm, S. (1980) *Biopolymers 19*, 31–36.

Block, R. E., Brady, A. M., & Joffe, S. (1973) *Biochem. Biophys. Res. Commun. 54*, 1595–1602.

Boggs, J. M., & Moscarello, M. A. (1984) *Can. J. Biochem. 62*, 11–18.

Calvin, M., Hermans, J., Jr., & Scheraga, H. A. (1959) *J. Am. Chem. Soc. 81*, 5048–5050.

Cammer, W., Bloom, B. R., Norton, W. T., & Gordon, S. (1978) *Proc. Natl. Acad. Sci. U.S.A. 75*, 1554–1558.

Campagnoni, A. T., Whitehead, D. T., & Rowan, R., III (1978) in *Biomolecular Structure and Function* (Agris, P. F., Ed.) pp 413–421, Academic Press, New York.

Carey, P. R. (1982) in *Biochemical Applications of Raman and Resonance Raman Spectroscopies*, pp 76–98, Academic Press, New York.

Deber, C. M., Moscarello, M. A., & Wood, D. D. (1978) *Biochemistry 17*, 898–903.

Deibler, G. E., Martenson, R. E., & Kies, M. W. (1972) *Prep. Biochem. 2*, 139–165.

Einstein, E. R., Csejtey, J., Dalal, K. D., Adams, C. W. M., Bayliss, D. B., & Hallpike, J. F. (1972) *J. Neurochem. 19*, 653–662.

Feinstein, M. B., & Felsenfeld, H. (1975) *Biochemistry 14*, 3049–3056.
Fritz, R. B., Chou, C.-H. J. (1983) *J. Immunol. 130*, 2180–2182.
Hamodrakas, S. J., Asher, S. A., Mazur, G. D., Regier, J. C., & Kafatos, F. C. (1982) *Biochim. Biophys. Acta 703*, 216–222.
Hashim, G. A. (1982) *Protides Biol. Fluids 30*, 187–191.
Krimm, S. (1962) *J. Mol. Biol. 4*, 528–540.
Krimm, S., & Bandekar, J. (1980) *Biopolymers 19*, 1–29.
Lagant, P., Vergoten, G., Fleury, G., & Loucheux-Lefebvre, M.-H. (1984) *Eur. J. Biochem. 139*, 149–154.
Lavialle, F., Adams, R. G., & Levin, I. W. (1982) *Biochemistry 21*, 2305–2312.
Liebes, L. F., Zand, R., & Phillips, W. D. (1975) *Biochim. Biophys. Acta 405*, 27–39.
Liebes, L. F., Zand, R., & Phillips, W. D. (1976) *Biochim. Biophys. Acta 427*, 392–409.
Lippert, J. L., Tyminski, D., & Desmeules, P. J. (1976) *J. Am. Chem. Soc. 98*, 7075–7080.
Margetson, S. A., Moore, W. J., & Gibbons, W. A. (1981) *Aust. J. Chem. 34*, 1373–1394.
Martenson, R. E. (1980) in *Biochemistry of Brain* (Kumar, S., Ed.) pp 49–79, Pergamon Press, Oxford and New York.
Martenson, R. E. (1981) *J. Neurochem. 36*, 1543–1560.
McClure, W. O., & Edelman, G. M. (1966) *Biochemistry 5*, 1908–1919.
McClure, W. O., & Edelman, G. M. (1967) *Biochemistry 6*, 559–566.
Mendz, G. T., Moore, W. J., & Carnegie, P. R. (1982) *Biochem. Biophys. Res. Commun. 105*, 1333–1340.
Miyazawa, T., & Blout, E. R. (1961) *J. Am. Chem. Soc. 83*, 712–719.
Parker, C. A. (1968) in *Photoluminescence of Solutions*, p 222, Elsevier, Amsterdam.
Pezolet, M., Pigeon-Gosselin, M., & Coulombe, L. (1976) *Biochim. Biophys. Acta 453*, 502–512.
Ruegg, M., Metzger, V., & Susi, H. (1975) *Biopolymers 14*, 1465–1471.
Sadikot, H., & Moore, W. J. (1983) *Aust. J. Chem. 36*, 33–41.
Schellman, J. A., & Schellman, C. (1964) *Proteins (2nd Ed.) 2*, 96–111.
Schiffer, M., & Edmundson, A. B. (1967) *Biophys. J. 7*, 121–135.
Siamwiza, M. N., Lord, R. C., Chen, M. C., Takamatsu, T., Harada, I., Matsuura, H., & Shimanouchi, T. (1975) *Biochemistry 14*, 4870–4876.
Smith, R. (1980) *Biochemistry 19*, 1826–1831.
Smith, R. (1982) *Biophys. Chem. 16*, 347–354.
Stoner, G. (1984) *J. Neurochem. 43*, 433–447.
Susi, H. (1972) *Methods Enzymol. 26*, 455–472.
Susi, H., Timasheff, S. N., & Stevens, L. (1967) *J. Biol. Chem. 242*, 5460–5466.
Swann, R. W., & Li, C. H. (1979) *Int. J. Pept. Protein Res. 14*, 494–503.
Timasheff, S. N., & Susi, H. (1966) *J. Biol. Chem. 241*, 249–251.
Turner, D. C., & Brand, L. (1968) *Biochemistry 7*, 3381–3390.
Vacher, M., Nicot, C., Pflumm, M., Luchins, J., Beychok, S., & Waks, M. (1984) *Arch. Biochem. Biophys. 231*, 86–94.
Vincent, J. S., Steer, C. J., & Levin, I. W. (1984) *Biochemistry 23*, 625–631.
Whitaker, J. N. (1982) *J. Immunol. 129*, 2729–2733.
Whitaker, J. N., Lisak, R. P., & Bashir, R. M. (1980) *Ann. Neurol. 7*, 58–64.
Yu, N.-T., Jo, B. H., & O'Shea, D. C. (1973) *Arch. Biochem. Biophys. 156*, 71–76.
Zand, R., & Agrawal, K. (1980) *Trans. Am. Soc. Neurochem. 11*, 242.